# MODELS FOR THE PREDICTION OF INSTANTANEOUS CUTTING FORCES IN END MILLING

Anna Carla Araujo, José Luis Lopes Silveira

COBEM 99
XV Congresso Brasileiro de Engenharia Mecânica
15th Brazilian Congress of Mechanical Engineering
22 - 26 de Novembro de 1999 / November 22 - 26, 1999 Águas de Lindóia, São Paulo,

# MODELS FOR THE PREDICTION OF INSTANTANEOUS CUTTING FORCES IN END MILLING

**Anna Carla Araujo**
**José Luís Silveira**
Universidade Federal do Rio de Janeiro, EE/COPPE
P.O. Box 68503 – 21945-970 – Rio de Janeiro, RJ, Brazil.
annacarla@serv.com.ufrj.br — jluis@serv.com.ufrj.br

***Abstract.*** *This work compares some of the available models for prediction of instantaneous forces in end milling. A cutting model for predicting the instantaneous milling forces involves partitioning each tooth cutting edge into a series of elemental tools. Based on this concept, the cutting forces on disc-like elements that comprise the end mill can be summed to give the total cutting force. Models based on empirical constants, orthogonal cutting data and oblique cutting relations are reviewed, proposed and compared.*

***Keywords:*** *Cutting forces, End milling, Machining*

## 1. INTRODUCTION

Machining is one of the oldest process for shaping components and due to its versatility and precision achieved through continual innovation, research and development, has become an indispensable process used in manufacturing industry. The need to understand the metal cutting processes have attracted the attention of many researchers which proposed different forms of modeling machining: analytical, numerical, experimental and hybrid approaches (Ehmann, Kapoor & DeVor, 1997). Some of the existing milling forces approaches are: the instantaneous rigid force models, instantaneous force models with static deflection, average rigid force models and regenerative dynamic force models (Smith and Tlusty, 1991).

In this paper, we consider the methods for prediction of forces in end milling which involves instantaneous rigid forces and classified them as: semi-empirical, mechanistic, orthogonal and oblique methods.

## 2. END MILLING MODELING

The machining process of end milling is shown in Fig. 1, which presents two moments of cutting: on the left, the tool is beginning to cut the workpiece and the cutting width

($a$) changes with the feed per tooth ($s_z$), so the average force increases in time; on the right, the cutting width ($a$) is constant and the force is periodic.

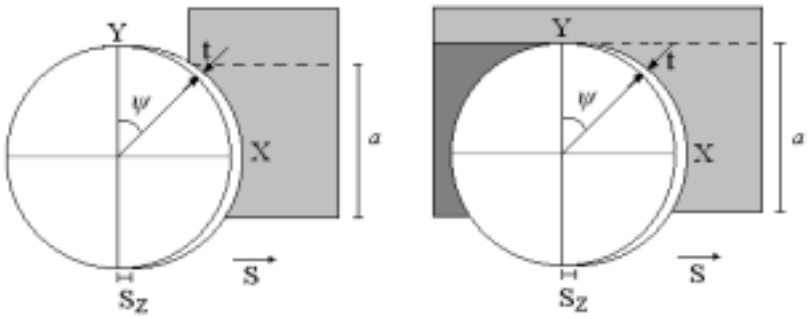


Figure 1 – End Milling.

The undeformed chip thickness ($t$) for each point of the cutting edge (Fig. 1) can be calculated from the expression (1) as a function of the angular position ($\psi$) of the point and the feed per tooth.

$$t = s_z \ \sin(\psi) \tag{1}$$

The geometry of the end mill and the important variables are shown in Fig. 2, in which is presented a lateral view of the tool-workpiece pair and the lateral face of the tool in contact with the workpiece unfolded (unrolled) in a plane together with the superior view of the tool.

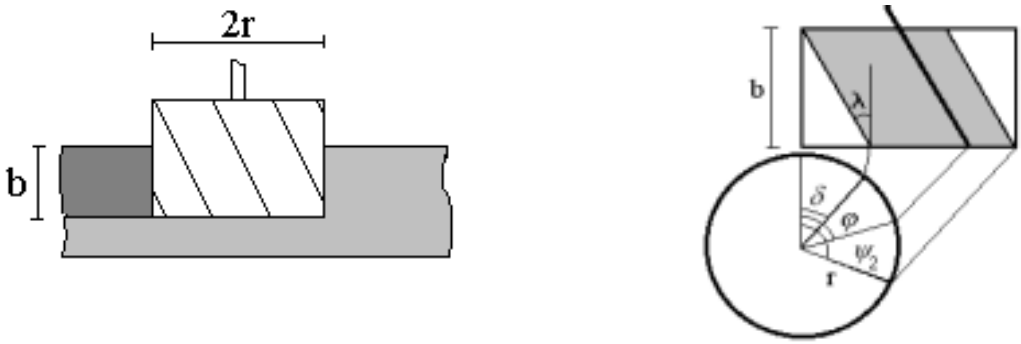


Figure 2 – Geometry of cut.

In Figure 2, the cutting edge of each tooth is represented by a line, inclined by the helix angle $\lambda$ on the plane and, on the superior view, the cutting edge is represented by the angle $\varphi$, which indicates the leading point of the cutting edge. The angle $\psi$ represents the position of each point of the cutting edge in contact with the workpiece. This way, the range for $\psi$ is from $\psi_1$, the initial angle, which in this case is zero, to $\psi_2$, the exit angle. The difference between them can be called the contact angle $\psi_o = \psi_2 - \psi_1$.

Other angles have to be defined: the angle $\delta$ is the difference between the angle $\psi$ of the leading point of the cutting edge and the last point of the edge which is engaged in the cut. The helix angle $\lambda$ relates the cutting edge and the $\psi$ angle, so an element of the cutting edge ($db$) can be written as:

$$db = \frac{r}{tg\lambda}\, d\psi \tag{2}$$

Each cutting edge passes, from $\psi_1$ to $\psi_2$, through three phases: phase A, the cutter is entering the workpiece and each rotation $d\psi$ increases the length of the edge engaged in cutting; phase B, the length of the cutting edge is constant; and in phase C it is decreasing. Moreover, depending on the relation between the contact angle $\psi_o$ and the $\delta$ angle, the geometry of the unfolded surface of cut can be classified as **Type I**, if the contact angle $\psi_o$ is larger than $\delta$, else it is called **Type II**.

In the following table are presented the ranges of $\varphi$ and $\psi$ of each region and each type of cutting.

Table 1 – Ranges of $\varphi$ and $\psi$

| | **Type I** | | **Type II** | | **Type I** | | **Type II** | |
|---|---|---|---|---|---|---|---|---|
| Region | $\varphi_{initial}$ | $\varphi_{final}$ | $\varphi_{initial}$ | $\varphi_{final}$ | $\psi_{initial}$ | $\psi_{final}$ | $\psi_{initial}$ | $\psi_{final}$ |
| A | $\psi_1$ | $\delta$ | $\psi_1$ | $\psi_2$ | $\psi_1$ | $\varphi$ | $\psi_1$ | $\varphi$ |
| B | $\delta$ | $\psi_2$ | $\psi_2$ | $\delta$ | $\varphi - \delta$ | $\varphi$ | $\psi_1$ | $\psi_2$ |
| C | $\psi_2$ | $\psi_2+\delta$ | $\delta$ | $\psi_2+\delta$ | $\varphi - \delta$ | $\psi_2$ | $\varphi - \delta$ | $\psi_2$ |

In general, the cutting forces in the end milling can be expressed as a function of chip thickness and depth of cut:

$$F = K\ t\ b \tag{3}$$

where $K$ is the specific cutting force, an empirical function of the workpiece material, tool geometry and the average chip thickness. Replacing the chip thickness, an element of the tangential and radial forces can be expressed as:

$$dF_t = K_t\, s_z\ \sin\psi\, db \qquad\qquad dF_r = K_r\, s_z\ \sin\psi\, db \tag{4}$$

Integrating in the ranges of $\psi$, on each cutting region (Table 1), and transforming to the workpiece referential, the forces acting can be written from (1) to (4), as:

$$\mathbf{F_n} = \begin{bmatrix} F_x \\ F_y \end{bmatrix}_n = \int_{\psi_1}^{\psi_2} s_z\ \sin\psi\, \frac{r}{tg\lambda} \begin{bmatrix} \cos\psi & \sin\psi \\ -\sin\psi & \cos\psi \end{bmatrix} \begin{bmatrix} -K_t \\ K_r \end{bmatrix} d\psi \tag{5}$$

The sum on all cutters results the total force:

$$\mathbf{F} = \sum_{n=1}^{N} \mathbf{F_n} \tag{6}$$

## 3. SEMI-EMPIRICAL MODELS

Koenigsberger and Sabberwal (Ehmann *et al.*, 1997) proposed a model (eq. 3) for tangential forces based on measurements during cutting tests and developed empirical coefficients that relate the instantaneous forces to the chip area in milling.

Tlusty and McNeil (1975) used an approach in which tangential and radial forces on the cutter were predicted based on Sabberwal model and using a fixed rate between these forces. The following equations describes the differential formulas for the forces where

$K_t^{(1)}$ is the tangential specific cutting force, and the superscript (1) indicates the first formulation to the forces.

$$dF_t^{(1)} = K_t^{(1)}\, t\, db \qquad\qquad dF_r^{(1)} = 0.3\, dF_t^{(1)} \tag{7}$$

In the special case of end milling, and from eq. (5), the forces on the workpiece referential, predicted by Tlusty, are:

$$\begin{bmatrix} dF_x^{(1)} \\ dF_y^{(1)} \end{bmatrix}_n = -\begin{bmatrix} \cos\psi + 0.3\, \sin\psi \\ 0.3\, \cos\psi - \sin\psi \end{bmatrix} dF_t^{(1)} \tag{8}$$

$$\begin{bmatrix} dF_x^{(1)} \\ dF_y^{(1)} \end{bmatrix}_n = -K_t^{(1)}\, s_z\, \frac{r}{\mathrm{tg}\,\beta} \int_{\psi_1}^{\psi_2} \begin{bmatrix} \sin\psi\, \cos\psi + 0.3\, \sin^2\psi \\ \sin^2\psi - 0.3\, \sin\psi\, \cos\psi \end{bmatrix} d\psi \tag{9}$$

Ber, Rotberg & Zombach (1988) introduced the vertical force and have considered the vertical and radial forces proportional to the tangential force as Tlusty have already done with the radial force:

$$dF_t^{(2)} = K_t^{(2)}\, t\, db \qquad dF_r^{(2)} = 0.4\, K_t^{(2)}\, t\, db \qquad dF_z^{(2)} = 0.3\, K_t^{(2)}\, t\, db \tag{10}$$

$$\begin{bmatrix} dF_x^{(1)} \\ dF_y^{(1)} \\ dF_z^{(1)} \end{bmatrix}_n = -K_t^{(2)}\, s_z\, \frac{r}{\mathrm{tg}\,\beta} \int_{\psi_1}^{\psi_2} \begin{bmatrix} \sin\psi\, \cos\psi + 0.4\, \sin^2\psi \\ \sin^2\psi - 0.4\, \sin\psi\, \cos\psi \\ 0.3\, \sin\psi \end{bmatrix} d\psi \tag{11}$$

## 4. MECHANISTICAL MODELS

The mechanistic models for the prediction of forces consider that the specific cutting force varies with the chip thickness as shown by Sabberwal (Kline *et al.*, 1981).

Kline, DeVor and Lindberg (1981) proposed an approximation of the specific force $K_t^{(3)}$ as a function of the feed rate $s_z$:

$$K_t^{(3)} = C_t\, (t)^p \cong C_t\, (s_z)^p \tag{12}$$

$$dF_t^{(3)} = C_t\, (s_z)^{p+1}\, \sin\psi\, db \qquad dF_r^{(3)} = K_r^{(3)}\, s_z\, \sin\psi\, db \tag{13}$$

where the value of $p$ is obtained experimentally, usually $p = -0.3$, and the values of $C_t$ and $K_r^{(3)}$ are constants for each material and cutting condition.

Altintas & Spence (1991) consider both $K_t^{(4)}$ and $K_r^{(4)}$ a function of the average chip thickness.

$$K_t^{(4)} = C_t\, (\bar{t})^{p_t} \qquad K_r^{(4)} = C_r\, (\bar{t})^{p_r} \tag{14}$$

where $C_t$, $C_r$, $p_t$ and $p_r$ are empirical constants and the average chip thickness is calculated using the expression:

$$\bar{t} = \frac{\sum_{n=1}^{N} (\cos\psi_i - \cos\psi_f)\, s_z}{\sum_{n=1}^{N} (\psi_f - \psi_i)} \tag{15}$$

So the forces predicted are:

$$dF_t^{(4)} = C_t\,(\bar{t})^{p_t+1}\,db \qquad\qquad dF_r^{(4)} = C_r\,(\bar{t})^{p_r+1}\,db \tag{16}$$

## 5. ORTHOGONAL CUTTING MODELS

Most practical cutting operations, such as milling, involves edges inclined at various angles to the direction of cut. The basic mechanism of cutting can be explained by analyzing cutting with a single cutting edge. The simplest case in which the cutting edge is perpendicular to the relative cutting velocity between tool and workpiece is called orthogonal cutting (Fig. 3) case which the forces can be analyzed in the plane of deformation. The following figure presents the important angles related to the orthogonal cutting: the shear plane angle $\phi$, the friction angle $\beta$, which is the angle between the resultant force and the normal to the rake face, and the tool rake angle $\gamma$.

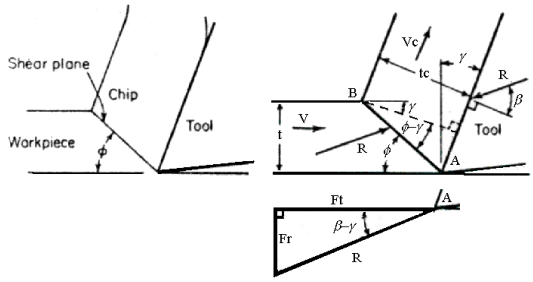


Figure 3 – Orthogonal cutting.

The Merchant analysis (Armarego, 1969) uses a thin-shear-plane model, which considers the plastic zone as a plane. To formulate the model some assumptions have been done: the sharpness of the tool tip, there is no rubbing, ploughing or side spread, the stresses are uniformly distributed on the shear plane and the modulus and direction of the resultant force on the contact between tool and chip are equal to the force applied in the shear plane. From these hypotheses and some geometrical relations, the expressions for tangential and radial forces were derived.

$$dF_t^{(5)} = \frac{\tau\cos(\beta-\gamma)}{\sin(\phi)\cos(\phi+\beta-\gamma)}\,t\,db = K_t(\beta,\phi,\gamma)^{(5)}\,t\,db \tag{17}$$

$$dF_r^{(5)} = \frac{\tau\sin(\beta-\gamma)}{\sin(\phi)\cos(\phi+\beta-\gamma)}\,t\,db = K_r(\beta,\phi,\gamma)^{(5)}\,t\,db \tag{18}$$

where $\tau$ is the stress on the shear plane.

Spence and Elbestawi (1998) used this expression with constant empiric values for $\beta$, and $\phi$. Usui, Hirota and Masuko (1978) developed experimental relations for $\beta$, and $\phi$ as a function of $\gamma$:

$$\phi(\gamma) = \exp\left(C_1\,\gamma - C_2\right) \qquad\qquad \beta(\gamma) = \exp\left(C_3\,\gamma - C_4\right) \tag{19}$$

where $C_1$, $C_2$, $C_3$ e $C_4$ are empirical constants. Using (19), equations (17) and (18) are rewritten as:

$$dF_t^{(6)}(\gamma) = K_t(\gamma)^{(6)}\,t\,db \qquad\qquad dF_r^{(6)}(\gamma) = K_r(\gamma)^{(6)}\,t\,db \tag{20}$$

The shear angle is a metal cutting characteristic which defines the deformation configuration. Merchant considered that $\tau$ would have the value of the yield shear stress for the work material and that the friction angle can be determined by the coefficient of friction, ($\mu = \text{tg } \beta$), from the usual dry sliding friction. To determine $\phi$ he assumed that the minimum-energy principle applied in metal cutting, so that the deformation process adjusted itself to a minimum-energy condition by equating $dF_p/d\phi$ to zero, for constant speed:

$$\phi = \frac{\pi}{4} - \frac{1}{2}(\beta - \gamma) \tag{21}$$

Using (21), the cutting forces (17) and (18) can be expressed as:

$$dF_t^{(7)} = 2\,\tau\,\text{cotg}(\phi)\,t\,db = K_t(\phi)^{(7)}\,t\,db \tag{22}$$

$$dF_r^{(7)} = 2\,\tau\,(\text{cotg}^2(\phi) - 1)\,t\,db = K_r(\phi)^{(7)}\,t\,db \tag{23}$$

The shear angle can be also determined experimentally knowing the chip-thickness ratio ($r = t/t_c$), assuming that the work material is incompressible and no side spread occurs. From the geometry of cut, it can be shown that:

$$\frac{t}{\text{sin}\phi} = \frac{t_c}{\cos(\phi - \gamma)} \qquad \text{and} \qquad \phi = \text{arctg}\left(\frac{r\,\cos\gamma}{1 - r\,\text{sin}\gamma}\right) \tag{24}$$

The forces (17) and (18) can be determined using this expression for $\phi$. Hence:

$$dF_t^{(8)} = K_t(\beta, r, \gamma)^{(8)}\,t\,db \qquad dF_r^{(8)} = K_r(\beta, r, \gamma)^{(8)}\,t\,db \tag{25}$$

## 6. OBLIQUE CUTTING MODELS

The mechanics of oblique cutting is based on a thin-shear-plane model as in Merchant analysis on the orthogonal cutting. The principal angle that characterizes the oblique cutting is the angle between the cutting edge and a normal to the cutting velocity vector, the angle of inclination or obliquity, which in end milling is equal to the helix angle ($\lambda$). The chip-flow angle ($\eta_c$) indicates the angle between the chip-flow velocity and the normal of the cutting edge, in the plane of the rake face and can be considered are collinear to the friction force angle ($\eta_c'$) (Armarego, 1969). The angles on oblique cutting are similar to those on orthogonal cutting measured on the plane containing the cutting velocity vector and the chip flow vector. The Figure 4 presents the principal angles: normal angles $\beta_n$, $\gamma_n$, $\phi_n$, the chip flow angle $\eta_c$ and helix angle $\lambda$. The relations between $\beta_n$, $\phi_n$ and $\beta$ are :

$$\text{tg}\,\beta_n = \text{tg}\,\beta\cos\eta_c \qquad \text{tg}\,(\beta_n + \phi_n) = \frac{\text{tg}\,\lambda\,\cos\gamma_n}{\text{tg}\,\eta_c - \text{sin}\,\gamma_n\,\text{tg}\,\lambda}, \tag{26}$$

Knowing these relations, the eq. (27) to (29) presents the force components as a function of $\beta$, $\beta_n$, $\lambda$, $\gamma_n$:

$$dF_t^{(9)} = \frac{\tau\,[\cos(\beta_n - \gamma_n) + \text{tg}\,\lambda\,\text{tg}\,\eta_c\,\text{sin}\,\beta]}{\text{sin}\,\phi_n\sqrt{\cos^2(\phi_n + \beta_n - \gamma_n) + \text{tg}^2(\eta_c)\,\text{sin}^2(\beta_n)}}\,t\,db = K_t^{(9)}\,t\,db \tag{27}$$

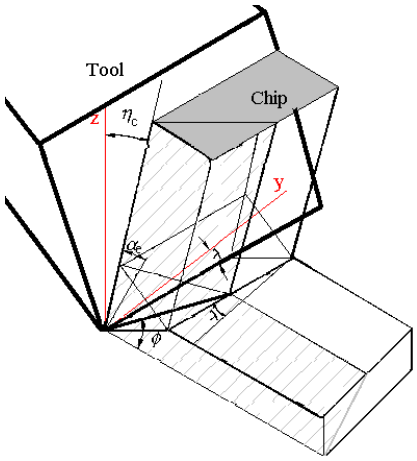


Figure 4 – Oblique cutting.

$$dF_r^{(9)} = \frac{\tau\,[\cos(\beta_n - \gamma_n)]}{\sin\phi_n\ \cos\lambda\ \sqrt{\cos^2(\phi_n + \beta_n - \gamma_n) + \mathrm{tg}^2(\eta_c)\ \sin^2(\beta_n)}}\ t\ db = K_r^{(9)}\ t\ db \tag{28}$$

$$dF_z^{(9)} = \frac{\tau\,[\cos(\beta_n - \gamma_n)\,\mathrm{tg}\,\lambda - \mathrm{tg}\,\eta_c\ \sin\beta_n]}{\sin\phi_n\ \sqrt{\cos^2(\phi_n + \beta_n - \gamma_n) + \mathrm{tg}^2(\eta_c)\ \sin^2(\beta_n)}}\ t\ db = K_z^{(9)}\ t\ db \tag{29}$$

Kronemberg (Armarego, 1969) assumed that the chip flow direction was in the velocity rake plane so that $\mathrm{tg}\,\eta_c = \mathrm{tg}\,\lambda\ \sin\gamma_n$ and $\beta_n + \phi_n = \frac{\pi}{2}$ and then the forces can be expressed as:

$$dF_t^{(10)} = \frac{\tau\,[\cos(\beta_n - \gamma_n) + \mathrm{tg}^2\lambda\ \sin\gamma_n\ \sin\beta]}{\sin\beta_n\ \sqrt{\cos^2(\gamma_n) + \mathrm{tg}^2\lambda\ \sin\gamma_n\ \sin^2(\beta_n)}}\ t\ db = K_t^{(10)}\ t\ db \tag{30}$$

$$dF_r^{(10)} = \frac{\tau\,[\cos(\beta_n - \gamma_n)\ \cos\lambda]}{\sin\beta_n\sqrt{\cos^2(\gamma_n) + \mathrm{tg}^2\lambda\ \sin\gamma_n\ \sin^2(\beta_n)}}\ t\ db = K_r^{(10)}\ t\ db \tag{31}$$

$$dF_z^{(10)} = \frac{\tau\,[\cos(\beta_n - \gamma_n)\,\mathrm{tg}\,\lambda - \mathrm{tg}\,\lambda\ \sin\gamma_n\ \sin\beta_n]}{\sin\beta_n\ \sqrt{\cos^2(\gamma_n) + \mathrm{tg}^2\lambda\ \sin\gamma_n\ \sin^2(\beta_n)}}\ t\ db = K_z^{(10)}\ t\ db \tag{32}$$

Stabler (Armarego, 1969) claimed that experimental evidence indicated a simple relationship where $\eta_c = \lambda$ for $\gamma_n$ between $-10^0$ and $10^0$. Then, $\mathrm{tg}\,(\beta_n + \gamma_n) = \frac{cos(\gamma_n)}{1 - sin\gamma_n}$ and so:

$$dF_t^{(11)} = \frac{\tau\,[\cos(\beta_n - \gamma_n) + \mathrm{tg}^2\lambda\ \sin\beta]}{\sin\phi_n\sqrt{\cos^2(\phi_n + \beta_n - \gamma_n) + \mathrm{tg}^2\lambda\ \sin^2(\beta_n)}}\ t\ db = K_t^{(11)}\ t\ db \tag{33}$$

$$dF_r^{(11)} = \frac{\tau\,[\cos(\beta_n - \gamma_n]\ \cos\lambda}{\sin\phi_n\sqrt{\cos^2(\phi_n + \beta_n - \gamma_n) + \mathrm{tg}^2\lambda\ \sin^2(\beta_n)}}\ t\ db = K_r^{(11)}\ t\ db \tag{34}$$

$$dF_z^{(11)} = \frac{\tau\,[\cos(\beta_n - \gamma_n)\,\mathrm{tg}\,\lambda - \mathrm{tg}\,\eta_c\ \sin\beta_n]}{\sin\phi_n\sqrt{\cos^2(\phi_n + \beta_n - \gamma_n) + \mathrm{tg}^2\lambda\ \sin^2(\beta_n)}}\ t\ db = K_z^{(11)}\ t\ db \tag{35}$$

Altintas & Lee (1996) and Armarego & Deshpande (1989) considered that the cutting force can be analyzed as a sum of two parcels, the cutting force and the edge force:

$$dF = dF_{cutting} + dF_{edge} \tag{36}$$

For Altintas & Lee (1996) the chip-thickness ratio ($r$) and the normal friction angle ($\beta_n$) were obtained from empirical relations of orthogonal data as a function of $\gamma_n$:

$$\beta_n(\gamma_n) = 19,1 + 0,29\gamma_n \qquad r(\gamma_n) = p(\gamma_n)\, t^q(\gamma_n) \tag{37}$$

where

$$p(\gamma_n) = 1,755 - 0,0282\gamma_n \qquad q(\gamma_n) = 0,331 - 0,0082\gamma_n \tag{38}$$

Then the tangential force $dF_t^{(12)}$, radial force $dF_r^{(12)}$, and axial force $dF_z^{(12)}$ can be calculated as:

$$dF_t^{(12)}(\phi) = \left(K_{te}^{(12)} + K_{tc}^{(12)}\, t\right)\, t\, db \tag{39}$$

$$dF_r^{(12)}(\phi) = \left(K_{re}^{(12)} + K_{rc}^{(12)}\, t\right)\, t\, db \tag{40}$$

$$dF_z^{(12)}(\phi) = \left(K_{ze}^{(12)} + K_{zc}^{(12)}\, t\right)\, t\, db \tag{41}$$

where the specific cutting forces are:

$$K_{tc}^{(12)} = K_t^{(9)} \qquad K_{rc}^{(12)} = K_r^{(9)} \qquad K_{zc}^{(12)} = K_z^{(9)} \tag{42}$$

and the specific edge forces $K_{te}^{(12)}$, $K_{re}^{(12)}$ and $K_{ze}^{(12)}$ are empirical constants.

For Armarego & Deshpande (1989) the values of $\beta$ and $r$ are constants and the specific edge forces are functions of the helix angle $\lambda$:

$$K_{te}^{(13)} = C_{te}\, \cos(\lambda) \qquad K_{re}^{(13)} = C_{re} \qquad K_{ze}^{(13)} = C_{ze}\, \cos(\lambda) \tag{43}$$

$$dF_t^{(13)}(\phi) = \left(K_{te}(\lambda)^{(13)} + K_{tc}^{(9)}\, t\right)\, t\, db \tag{44}$$

$$dF_r^{(13)}(\phi) = \left(K_{re}(\lambda)^{(13)} + K_{rc}^{(9)}\, t\right)\, t\, db \tag{45}$$

$$dF_z^{(13)}(\phi) = \left(K_{ze}(\lambda)^{(13)} + K_{zc}^{(9)}\, t\right)\, t\, db \tag{46}$$

## 7. A NEW PROPOSAL

Using the Armarego & Deshpande model (1989) and minimizing the cutting force energy to obtain the shear angle, the cutting force is given by:

$$dF_t^{(14)}(\phi) = \left(K_{te}(\lambda)^{(13)} + K_{tc}^{(14)}\, t\right)\, t\, db \tag{47}$$

$$dF_r^{(14)}(\phi) = \left(K_{re}(\lambda)^{(13)} + K_{rc}^{(14)}\, t\right)\, t\, db \tag{48}$$

$$dF_z^{(14)}(\phi) = \left(K_{ze}(\lambda)^{(13)} + K_{zc}^{(14)}\, t\right)\, t\, db \tag{49}$$

where the specific cutting forces are:

$$K_{tc}^{(14)} = K_t^{(9)}(\phi\,\big|_{\substack{min\\energy}}) \qquad K_{rc}^{(14)} = K_r^{(9)}(\phi\,\big|_{\substack{min\\energy}}) \qquad K_{zc}^{(14)} = K_z^{(9)}(\phi\,\big|_{\substack{min\\energy}}) \tag{50}$$

## 8. ANALYSIS AND COMPARATION

To compare those 14 models, with so many empirical constants, the data from the experimental work of Tlusty and MacNeil (1975) was taken as reference. The mill chosen has normal rake angle $\gamma_n = 9^o$, four cutting edges $z = 4$, helix angle $\lambda = 30^o$, contact angle $\varphi_o = 90^o$ and friction coefficient $\mu = 0.45$ ($\beta = 24,2^o$).

The models comparison are presented on Fig. 5. The first graphic in the left shows standard curves where the forces calculated from different models were divided by a constant to analyze the shape of the different curves. Only 12, 13 and 14 models differs from the standard behavior of the other 11 curves. This graphic is a detail of that at the botton, which shows almost one rotation of the end mill. The second graphic, in the right, shows another way to compare them, all curves were translated to the same minimum point where the actual amplitude of each one can be compared. The average values and the difference between the maximum and minimum values ($\Delta$) of all 14 curves are shown on Table 2.

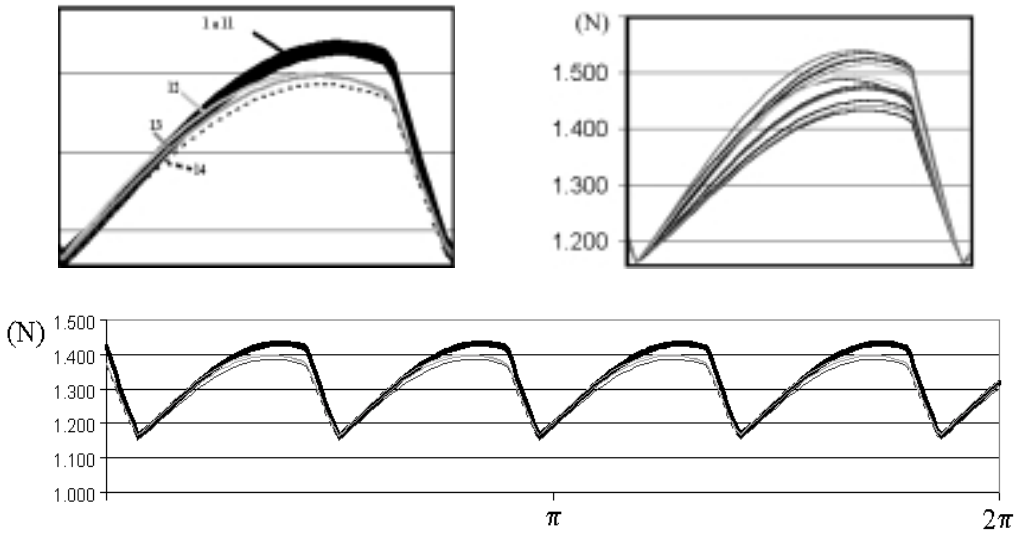


Figure 5 – Graphics of force from different models as a function of the rotation angle

Table 2 – Model number, Average Values and Amplitude $\Delta$ of Forces

| 1 | 2 | 3 | 4 | 5 | 6 | 7 | 8 | 9 | 10 | 11 | 12 | 13 | 14 |
|---|---|---|---|---|---|---|---|---|---|---|---|---|---|
| 1326 | 1425 | 1782 | 1782 | 1517 | 1826 | 1508 | 1536 | 1750 | 1397 | 1796 | 1827 | 1871 | 1540 |
| 273 | 290 | 367 | 367 | 313 | 376 | 311 | 317 | 355 | 281 | 365 | 328 | 334 | 380 |

## 9. CONCLUSION

In this work, some of the available models for prediction of instantaneous forces in end milling were compared. Most of the models presented a similar shape in the description of the force variation, the exeption were the models which included edge forces. A new proposal including edge forces and an energy approach for the cutting forces was presented and compared with the existing models.

## REFERENCES


Altintas, Y. & Lee, P., 1996, A General Mechanics and Dynamics Model for Helical End Mills, Annals of the CIRP, Vol. 45/1.

Altintas, Y. & Spence, A., 1991, End Milling force algorithms for CAD Systems, Annals of CIRP, Vol. 40/1, pp. 31-34.

Armarego, E.J. & Deshpande, N.P., 1991, Computerized end-milling forces prediction with cutting models allowing for eccentricity and cutter deflections, Annals of CIRP, Vol. 40/1, pp. 25-29.

Armarego, E.J. & Deshpande, N.P., 1989, Computerized predictive cutting models for forces in end-milling including eccentricity effects, Annals of CIRP, Vol. 38/1, pp. 45-49.

Armarego, E.J.A. & Deshpande, N.P., 1993, Force prediction models and CAD/CAM software for helical tooth milling process. I. Basic approach and cutting analyses, Int. J. Prod. Res., vol 31, no 8, pp. 1991-2009.

Armarego, E. J. A. & Brown, R. H., 1969, The machining of metals, Prentice-Hall, Inc. New Jersey.

Ber, A.; Rotberg, J. & Zombach, S., 1988, A method for cutting fore evaluation of end mills, Annals of CIRP, Vol. 37/1, pp. 37-40.

Ehmann, K. F. ; Kapoor, S. G. ; DeVor, R.E. & Lazoglu, I., 1997, Machining process modeling: a review, Journal of Manufacturing Science and Engineering, Vol 119, pp. 655-663.

Kline, W. ; DeVor, R. & Lindberg, J., 1982, The prediction of cutting forces in end milling with application to cornering cuts, Int. Mach. Tool. Des. Res., Vol 22, n.1, pp. 7-22.

Mounayri, H. ; Spence, A.D. & Elbestawi, M.A., 1998, Milling process simulation - a generic solid modeler based paradigm, Journal of Manufacturing Science and Engineering, Vol 120, pp. 213-221.

Tlusty , J. & MacNeil, 1975, Dynamics of cutting in end Milling, Annals of the CIRP, Vol. 24/1

Smith, S. & Tlusty, J., 1991, An Overview of Modeling and simulation of the milling process, Journal of Engineering for Industry, Vol 113, pp. 169-175.

Usui, E. ; Hirota, A. & Masuko, M., 1978, Analytical prediction of three dimensional cutting process, Journal of Engineering for Industry, Vol 100, pp. 222-228.